

# New mechanisms of void growth in Au–Al wire bonds: Volumetric shrinkage and intermetallic oxidation

H. Xu,<sup>a,\*</sup> C. Liu,<sup>b</sup> V.V. Silberschmidt,<sup>b</sup> S.S. Pramana,<sup>c</sup> T.J. White,<sup>c,d</sup> Z. Chen<sup>c</sup>  
and V.L. Acoff<sup>a</sup>

<sup>a</sup>Department of Metallurgical and Materials Engineering, The University of Alabama, Tuscaloosa, AL 35487, USA

<sup>b</sup>Wolfson School of Mechanical and Manufacturing Engineering, Loughborough University, Loughborough LE11 3TU, UK

<sup>c</sup>School of Materials Science and Engineering, Nanyang Technological University, Nanyang Avenue, Singapore 639798, Singapore

<sup>d</sup>Centre for Advanced Microscopy, Australian National University, Canberra ACT 2601, Australia

Received 16 June 2011; accepted 30 June 2011

Available online 8 July 2011

This letter examines void nucleation and coalescence in Au–Al wire bonds using high-resolution transmission electron microscopy. It is found that void formation is not only attributed to Kirkendall-type migration as conventionally believed, but also due to volumetric shrinkage and intermetallic oxidation. A volumetric shrinkage of a few percent is associated with intermetallic growth and phase transformations. Intermetallic oxidation occurs at the intermetallics/alumina interface and the migration of oxygen towards the intermetallics leads to void growth and thickening of the surrounding oxide walls.

© 2011 Acta Materialia Inc. Published by Elsevier Ltd. All rights reserved.

**Keywords:** Wire bonding; Void; Intermetallic compounds; Oxidation; Transmission electron microscopy (TEM)

Wire bonding is the primary method of making electrical interconnections between integrated circuits and external circuitry. It is the most cost-effective and flexible interconnect technology, and has been extensively adopted in semiconductor packages [1]. However, a critical issue remains with regard to the growth of voids in gold wire bonds, which essentially controls bond failure and durability. Although the interfacial evolution in Au–Al bonds [2–7] has been extensively investigated, a full account of the nucleation and coalescence of voids has not been published.

In the experiments, a gold wire (99.99 wt.%/20  $\mu\text{m}$  diameter) was bonded to an aluminum metallization pad (1  $\mu\text{m}$  thick) on a silicon chip using an ASM Eagle 60 ball/wedge automatic bonder. Bonding was complete in 0.008 s using a combination of transverse ultrasonic vibration (amplitude 612.5 nm/frequency 138 kHz), an external force normal to the interface (80 mN) and heat (175 °C). In order to accelerate void growth, samples were annealed at 175 °C to an accuracy of (2 °C in a vacuum furnace ( $10^{-3}$  Pa) for 1, 5, 9, 25, 49 and 100 h with an error of (2 min). Electron transparent cross-sections

of the Au–Al bonds were prepared with a dual-beam focused ion beam system (FEI Nova 600 NanoLab). Transmission electron microscopy (TEM) analysis was performed at 200 kV (JEOL 2100F). Fast Fourier transforms (FFT) of lattice images calculated using ImageJ 1.42q were employed to identify the intermetallic compounds (IMC).

Our previous study shows that the ubiquitous native alumina layer was fragmented during bonding, and Au<sub>4</sub>Al and AuAl<sub>2</sub> IMCs form that encapsulate alumina remnants [2]. Here, we found that a few nano-size voids are situated inside the large alumina debris (Fig. 1a), rather than at the IMC/metal interface. During aging, Au<sub>8</sub>Al<sub>3</sub> emerges as a third IMC between Au<sub>4</sub>Al and AuAl<sub>2</sub>, and gradually becomes the dominant phase. After the Al pad is consumed, AuAu<sub>2</sub> begins complete conversion to Au<sub>8</sub>Al<sub>3</sub>. Subsequently, Au<sub>8</sub>Al<sub>3</sub> reacts with Au to form Au<sub>4</sub>Al. TEM revealed that void growth is accompanied with the IMC evolution in Au–Al bonds. These voids coalesced during annealing (Fig. 1b and c), with excessive growth (Fig. 2) after 100 h at 175 °C. The voids are always surrounded by a thin layer of bright contrast (Figs. 1 and 2c), that high-resolution (HR) TEM and FFT (Fig. 2d) showed to be amorphous alumina and gold nanocrystals. In addition, there is an obvious increase in thickness of the oxide layer during

\* Corresponding author. Tel.: +1 205 3484473; e-mail addresses: [HXu14@bama.ua.edu](mailto:HXu14@bama.ua.edu); [HuiXu.hit@gmail.com](mailto:HuiXu.hit@gmail.com)

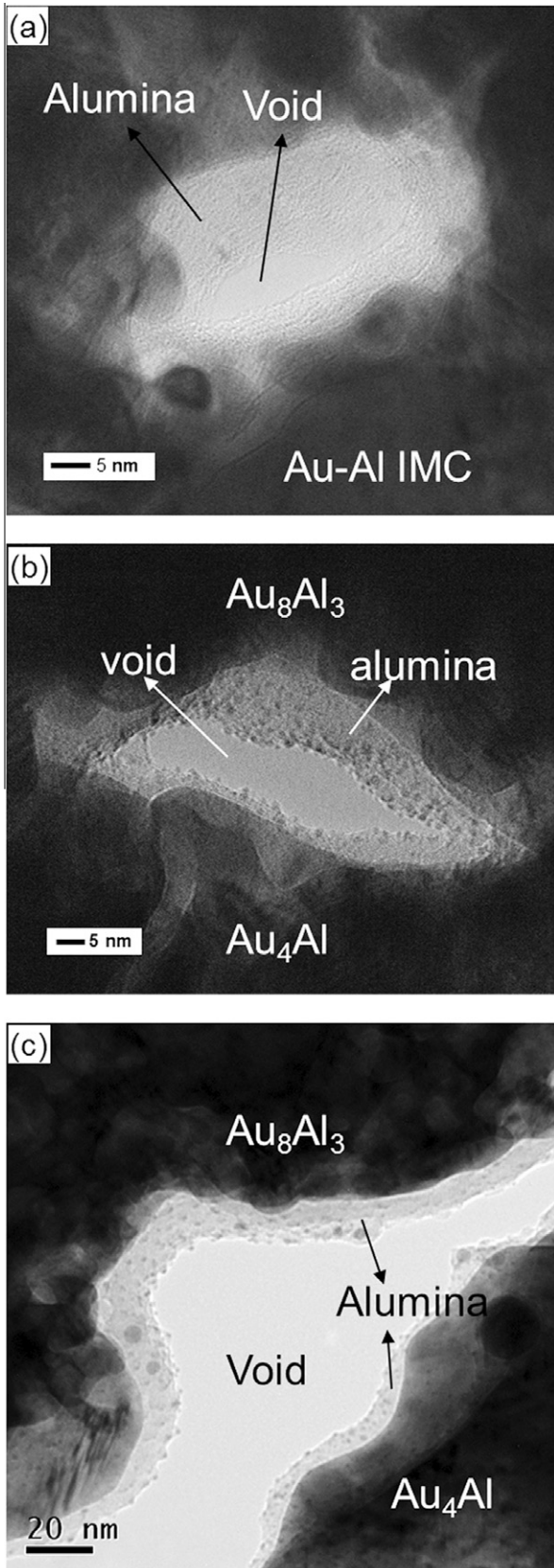


**Figure 1.** Evolution of voids and the neighboring oxide layer in Au–Al bond during annealing process. (a) A few voids formed in the center of large remnant alumina particles prior to annealing; (b) a void tens of nanometers in diameter after annealing for 5 h at 175 °C and (c) large voids of ~100 nm or more in diameter after annealing for 25 h at 175 °C.

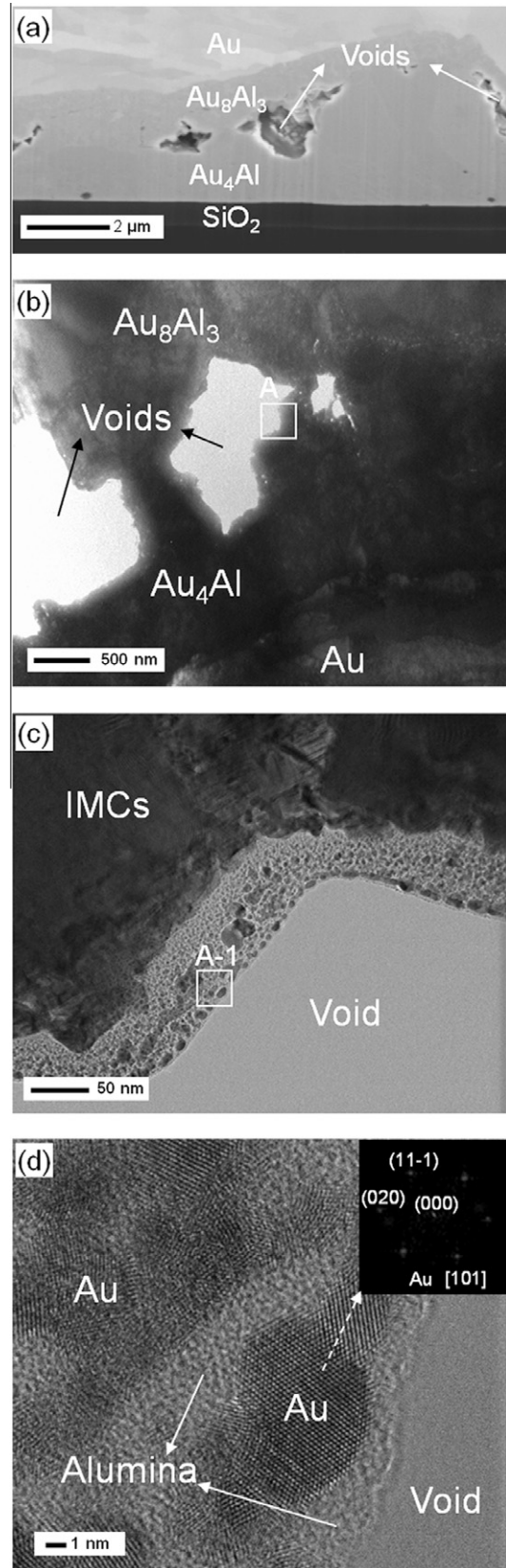


**Figure 2.** Au–Al bonds after annealing for 100 h at 175 °C: (a) scanning electron micrograph showing large voids inside IMCs; (b) TEM image showing voids a few micrometers in diameter; (c) HRTEM of region A in (b) showing a thin layer that surrounded the void; (d) lattice image of region A-1 in (c) indicating that the thin layer consisted of amorphous alumina and crystalline gold nanoparticles.

**Table 1.** Calculated molar volumes of Au–Al IMCs.

Phase	Compound symmetry	Space group	Unit cell volume ( $\text{\AA}^3$ )	Number of formula weights per unit cell	Molar volume ( $\text{cm}^3 \text{mol}^{-1}$ )
Au	fcc	<i>Fm-3m</i>	67.85	4	10.21
Al	fcc	<i>Fm-3m</i>	66.41	4	10.00
Au <sub>4</sub> Al	Cubic ( $\beta'$ )	<i>P2<sub>1</sub>3</i>	331.76	4	49.95
Au <sub>8</sub> Al <sub>3</sub>	Rhombohedral	<i>R-3c</i>	724.77	4	109.11
Au <sub>2</sub> Al	Orthorhombic	<i>Pnma</i>	190.54	4	28.68
	Orthorhombic	<i>Pmm</i>	475.16	10	28.61
AuAl	Cubic	<i>Pm-3m</i>	30.96	1	18.64
	Monoclinic	<i>P2<sub>1</sub>/m</i>	135.26	4	20.36
AuAl <sub>2</sub>	Cubic	<i>Fm-3m</i>	215.71	4	32.48

**Table 2.** Volume change associated with IMC formation and phase transformation in Au–Al bonds.

Reaction	Volume change (%)
Au + 2Al $\rightarrow$ AuAl <sub>2</sub>	+7.5
Au + Al $\rightarrow$ AuAl	-7.8
2Au + Al $\rightarrow$ Au <sub>2</sub> Al	-5.7
8Au + 3Al $\rightarrow$ Au <sub>8</sub> Al <sub>3</sub>	-2.3
4Au + Al $\rightarrow$ Au <sub>4</sub> Al	-1.8
3AuAl <sub>2</sub> + 13Au $\rightarrow$ 2Au <sub>8</sub> Al <sub>3</sub>	-5.2
Au <sub>8</sub> Al <sub>3</sub> + 4Au $\rightarrow$ 3Au <sub>4</sub> Al	-0.1

annealing, from 5 to 10 nm (5 h) to 10–20 nm (25 h) and to  $\sim$ 50 nm (100 h) (Figs. 1 and 2).

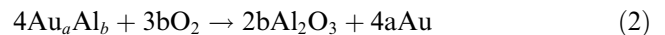
Void growth during annealing is usually attributed to Kirkendall porosity [8], i.e. the faster diffusing species create vacancies at a rate unmatched by vacancy filling. However, this study shows that voids are inside IMCs, but not at the metal and IMC interface. The supersaturation of vacancies, seen in miscible binary alloy systems where there is ready diffusion of either species, may not be possible in intermetallic systems, and therefore some mechanism rather than the Kirkendall one may be applicable to the growth of voids in Au–Al bonds during annealing.

Stephenson [9] proposed that large plastic stresses developed between product phases arising from significantly different specific volumes may initiate void formation between IMC layers. The molar volumes of IMCs can be calculated using:

$$V_m = V_c N_a / Z \quad (1)$$

where  $V_m$  is the molar volume of phase,  $V_c$  is the volume of the unit cell,  $N_a$  is the Avogadro constant ( $6.022 \times 10^{23} \text{mol}^{-1}$ ) and  $Z$  is the number of formula weights per unit cell (Table 1). Volume changes associated with intermetallic growth and phase transformation in Au–Al bonds are estimated using calculated molar volumes (Table 2). Except for AuAl<sub>2</sub>, the growth of other IMCs results in shrinkage. Since AuAl<sub>2</sub> is a thin transitional phase compared to other IMCs, its contribution to the whole volume change can be ignored. The entire volumetric shrinkage increases as Au<sub>8</sub>Al<sub>3</sub> and Au<sub>4</sub>Al grow during annealing, with stresses relieved by the initiation and propagation of voids at weak regions. However, the analysis of molar volumes shows that shrinkage is only a few percent, which in itself is insufficient to generate large voids (Fig. 2). Therefore, other factors must contribute to void growth.

The evolution of the void and the surrounding oxide layer with annealing time is schematically illustrated in Figure 3. Prior to annealing, the initial voids are surrounded by a thin alumina layer (5–10 nm thick) as seen in Figure 1a (illustrated in Fig. 3a). As annealing progresses, the thickness of this oxide layer,  $d$ , increases and the voids grow as in Figures 1b and c and 2 (illustrated in 3b and c), suggesting that an additional mechanism is involved. As proposed in Figure 3, this may be the migration of oxygen towards the Au–Al IMCs to enable the internal reaction.



where  $\text{Au}_a\text{Al}_b$  would be AuAl<sub>2</sub>, Au<sub>8</sub>Al<sub>3</sub> or Au<sub>4</sub>Al. Sritharan et al. [10] reported that the oxidation rate constant

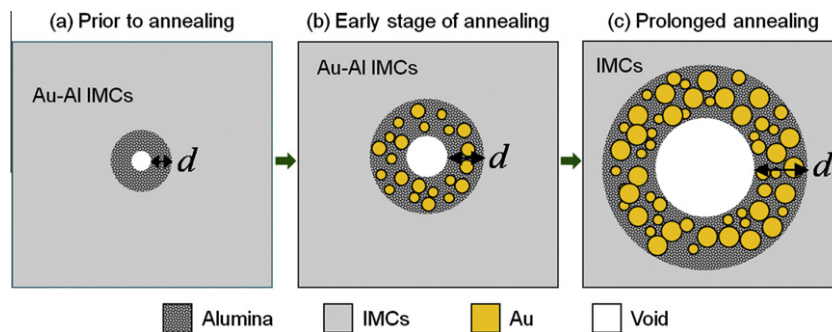
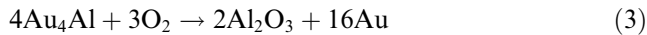


**Figure 3.** Illustration of evolution of voids and surrounding oxide layers in Au–Al bonds: (a) prior to annealing, the initial voids are surrounded by thin alumina layer (5–10 nm thick); (b) and (c) during annealing, crystalline Au nanoparticles emerge in alumina, and the thickness of the oxide layer,  $d$ , has increased.

of Au<sub>4</sub>Al was the largest among the Au–Al IMCs. Also, the fact that product Al<sub>2</sub>O<sub>3</sub> is always located near or inside Au<sub>4</sub>Al rather than other intermetallic phases suggests the favored oxidation of Au<sub>4</sub>Al. Thus, Eq. (2) can be specified as



Oxygen can potentially be supplied from non-stoichiometric alumina or the furnace atmosphere, although the partial pressure of O<sub>2</sub> may be very low in a vacuum furnace (10<sup>-3</sup> Pa). The Au reaction product could be sufficiently mobile to merge into crystalline nanoparticles (Fig. 3b and c), consistent with the observation of pure Au embedded in the oxide layer (Fig. 2c and d). This confirms that oxidation occurs at the IMCs/alumina interface and is consistent with previous studies of thin film and massive IMCs [10,11]. Migration of oxygen towards the IMCs leads to void growth and thickening of the surrounding oxide walls.

The validation of IMC oxidation mechanism is supported by the related phenomena in Cu–Al bonds. The alumina layer in Cu–Al bonds remains the same thickness and Cu nanoparticles are absent after annealing, suggesting less significance of Cu–Al IMC oxidation [12]. Thus, the voids are much less and smaller in Cu–Al bonds due to the lack of driving force of IMC oxidation.

It is noteworthy that the formation of large cavities up to 10 μm in the Au–Al bond after extended annealing at higher temperatures (e.g. 100 h at 250 °C) may also be attributed to the significant outward diffusion (Kirkendall-type migration) of Au to react with Al in the area beyond the perimeter of bonds, which is evidenced since a huge amount of IMCs formed outside the bonds. In contrast, the growth of Cu–Al IMCs is much slower than that of Au–Al IMCs, and almost no Cu–Al IMCs form beyond the bond edge, so the loss of the Cu in Cu–Al bonds is much less than the Au in Au–Al bonds.

In conclusion, we found that a few nanovoids form inside the large alumina debris during gold wire bond-

ing, and grow dramatically during annealing. Such voids are located within the IMCs rather than at the IMC/metal interface, suggesting that their growth is not only attributed to Kirkendall-type migration as conventionally believed. We proposed two new mechanisms, i.e. volumetric shrinkage and oxidation of IMCs, which together with Kirkendall mechanism account for void growth in Au–Al bonds. A volumetric shrinkage of a few percent is associated with intermetallic growth and phase transformations. Intermetallic oxidation occurs at the intermetallics/alumina interface and the migration of oxygen towards the intermetallics leads to void growth and thickening of the surrounding oxide walls in Au–Al bonds. In other bonds or joints where void growth affects their properties, volumetric shrinkage and IMC oxidation should also be considered as possible mechanisms.

- [1] G.G. Harman, *Wire Bonding in Microelectronics*, third ed., McGraw-Hill, New York, 2010.
- [2] H. Xu, C. Liu, V.V. Silberschmidt, S.S. Pramana, T.J. White, Z. Chen, M. Sivakumar, V.L. Acoff, *J. Appl. Phys.* 108 (2010) 113517.
- [3] J. Li, L. Han, J. Duan, J. Zhong, *J. Appl. Phys. Lett.* 90 (2007) 242902.
- [4] C. Xu, T. Sritharan, S.G. Mhaisalkar, *Scripta Mater.* 56 (2007) 549.
- [5] J. Qi, N.C. Hung, M. Li, D. Liu, *Scripta Mater.* 54 (2006) 293.
- [6] A. Karpel, G. Gur, Z. Atzmon, W. Kaplan, *J. Mater. Sci.* 42 (2007) 2347.
- [7] S. Murali, N. Srikanth, C.J. Vath III, *Mater. Lett.* 58 (2004) 3096.
- [8] C.D. Breach, F.W. Wulff, *Microelectron. Reliab.* 50 (2010) 1.
- [9] G.B. Stephenson, *Acta Metal et Mat.* 36 (1998) 2663.
- [10] T. Sritharan, Y.B. Li, C. Xu, S. Zhang, *J. Mater. Res.* 23 (2008) 1371.
- [11] C. Xu, C.D. Breach, T. Sritharan, F. Wulff, S.G. Mhaisalkar, *Thin Solid Films* 462–463 (2004) 357.
- [12] H. Xu, C. Liu, V.V. Silberschmidt, S.S. Pramana, T.J. White, Z. Chen, V.L. Acoff, *Acta Mater* 59 (2011) 5661.